



# Dynamic contrast-enhanced magnetic resonance imaging features and apparent diffusion coefficient value of HER2-positive/HR-negative breast carcinoma

Peipei Chen<sup>^</sup>, Suhong Zhao<sup>^</sup>, Weihua Guo<sup>^</sup>, Guangrui Shao<sup>^</sup>

Department of Radiology, The Second Hospital of Shandong University, Jinan, China

*Contributions:* (I) Conception and design: S Zhao, P Chen; (II) Administrative support: S Zhao; (III) Provision of study materials or patients: W Guo, G Shao; (IV) Collection and assembly of data: S Zhao; (V) Data analysis and interpretation: P Chen; (VI) Manuscript writing: All authors; (VII) Final approval of manuscript: All authors.

*Correspondence to:* Suhong Zhao, PhD. Department of Radiology, The Second Hospital of Shandong University, 247 Beiyuan Street, Tianqiao District, Jinan 250033, China. Email: jn8193303@163.com.

**Background:** According to hormone receptor (HR) status, human epidermal growth factor 2 positive (HER2+) breast carcinoma can be divided into HR- and HR+, with different treatment and prognosis. We analyzed the dynamic contrast-enhanced magnetic resonance imaging (DCE-MRI) findings, apparent diffusion coefficient (ADC) value and the combination of DCE-MRI and ADC value of HER2+/HR- breast carcinoma.

**Methods:** Totally 259 cases (96 HR-, 163 HR+) of pathologically verified HER2+ breast carcinoma were collected. Patients underwent DCE-MRI and diffusion weighted imaging (DWI). The morphological characteristics, internal enhancement characteristics, early enhancement rate (EER), and time-signal intensity curves (TIC) were recorded, and ADC values were measured. The relationship between each feature and HER2+/HR- breast cancer was analyzed. Area under the curves (AUC) was used to compare diagnostic performance of DCE-MRI, ADC value and the combination of DCE-MRI and ADC value.

**Results:** HER2+/HR- breast cancer presented as non-mass enhancement (NME), mass with NME, whereas HER2+/HR+ breast cancer presented as mass ( $P < 0.001$ ). HR- cases showed a round or oval shape with circumscribed margins, whereas HR+ cases showed an irregular mass with irregular or spiculated margins ( $P = 0.001$ ,  $P = 0.028$ ). The size of the mass, the internal enhancement characteristics, EER, and TIC did not differ significantly between the two HER2+ breast carcinomas. The ADC values for HR- and HR+ breast cancers were  $[1.2 (1.14, 1.33)] \times 10^{-3} \text{ mm}^2/\text{s}$  and  $[1.0 (0.89, 1.11)] \times 10^{-3} \text{ mm}^2/\text{s}$ , respectively, which were statistically significant ( $Z = -9.119$ ,  $P < 0.001$ ). The ADC value can be used for diagnosing HER2+/HR- breast carcinoma, with the threshold value of  $1.095 \times 10^{-3} \text{ mm}^2/\text{s}$  [negative predictive value (NPV) of 89.8%, sensitivity of 86.5% and specificity of 70.6%]. The AUCs of ADC value, DCE-MRI, and DCE-MRI combined with ADC value were 0.839, 0.689 and 0.860, respectively. AUC of the DCE-MRI combined with ADC value was significantly higher than DCE-MRI alone ( $P < 0.0001$ ).

**Conclusions:** The diagnostic performance of the DCE-MRI combined with ADC value was good in diagnosing HER2+/HR- breast cancers. MRI is an effective tool in diagnosing HER2+/HR- breast carcinoma, which will help select the clinical treatment plan and determine the prognosis.

<sup>^</sup> ORCID: Peipei Chen, 0000-0002-1817-5410; Suhong Zhao, 0000-0002-4541-9070; Weihua Guo, 0000-0001-6425-4964; Guangrui Shao, 0000-0001-5100-9134.

**Keywords:** Magnetic resonance imaging (MRI); breast carcinoma; human epidermal growth factor 2 (HER2); hormone receptors (HRs)

Submitted Nov 26, 2022. Accepted for publication Apr 23, 2023. Published online May 12, 2023.

doi: 10.21037/qims-22-1318

View this article at: <https://dx.doi.org/10.21037/qims-22-1318>

## Introduction

Breast carcinoma is one of the most common female malignant tumors, and human epidermal growth factor 2 positive (HER2+) breast carcinoma accounts for about 20% of invasive carcinomas (1). Hormone receptor (HR) status affects the survival and recurrence of HER2+ breast carcinoma (2). According to HR status, tumors can be divided into HER2+/HR- and HER2+/HR+ (3). HER2+/HR- breast carcinoma can be treated with targeted therapy and chemotherapy, whereas HER2+/HR+ patients also require endocrine therapy (3). The 5-year mortality is higher for HER2+/HR- breast cancer than for HER2+/HR+ tumors; however, neoadjuvant chemotherapy is more effective and the partial remission rate is higher in HER2+/HR- tumors (4). Although the molecular status of HR is mainly determined by biopsy, in approximately 20% of patients, receptor status after surgery is inconsistent with biopsy because of the heterogeneity of tumors (5). Accurate prediction of HER2+/HR- status before surgery would help clinicians choose the optimal treatment and improve the prognosis of patients.

Dynamic contrast enhanced magnetic resonance imaging (DCE-MRI) can reflect the dynamic distribution of contrast agent in the carcinoma and show the morphological and hemodynamic characteristics of the lesions (6). HER2+ breast cancer is characterized by irregular margins, multifocality, and an outflow curve (7), whereas HER2+/HR- breast cancer is characterized by a well-defined mass and non-mass enhancement (NME) (8).

Diffusion weighted imaging (DWI) is an additional technique of DCE-MRI that does not require enhancement, and is fast and cost-effective (9,10). DWI is the only method that allows MRI to detect water diffusion in tissues, which is quantitatively analyzed with the apparent diffusion coefficient (ADC) value, and a low ADC value indicates restricted diffusion (9,10). The ADC value does not differentiate between molecular subtypes of breast cancer (11).

The DCE-MRI findings of HER2+/HR- breast carcinoma have been reported previously (8), whereas fewer

studies have reported the ADC value or the combination of DCE-MRI and ADC value (12). The aim of our research was to analyze the DCE-MRI findings and ADC value of HER2+/HR- breast carcinoma to guide clinical treatment and prognosis evaluation.

## Methods

### Study patients

This retrospective research was approved by the ethics committee of the Second Hospital of Shandong University [No. KYLL-2021(LW)042] and the patient informed consent was waived due to the nature of the retrospective analysis. The study was conducted in accordance with the Declaration of Helsinki (as revised in 2013). Between January 2015 and March 2021, 259 women (average age, 50.75±10.35 years; age range, 25 to 79 years) with HER2+ breast cancer pathologically proven were included. All our patients underwent DCE-MRI and DWI examination before operation. Patients who were treated with radiotherapy and chemotherapy, with other molecular subtypes, whose scanned data were incomplete, and lesions that were too small (<0.5 cm) to measure ADC value were excluded.

### Magnetic resonance imaging (MRI)

Both breast MRI examinations were performed in a 3.0 T magnet (GE Healthcare, Discovery MR750), and the eight-channel dedicated breast coil was used. The patient was in prone position. Premenopausal females were examined during 7–14 days of the menstrual cycle. Conventional MRI and DWI were performed before DCE-MRI.

DCE-MRI was performed with axial T1-weighted three-dimensional dynamic gradient echo sequence (VIBRANT) with Dixon fat suppression (flip angle, 5°; TR, 3.9 ms; TE, 1.7 ms; matrix size, 348×348; field of view, 360×360 mm; and slice thickness, 1.8 mm). DCE images were acquired immediately after the gadodiamide (rate of 2 mL/s, 0.2 mmol/kg body weight) and saline injections. Seven

repeated DCE-MRI sequences were acquired consecutively, with each sequence having a duration of 60 s. DWI examination used axial echo-planar single shot STIR fat suppressed diffusion weighted sequence with b-values of 0 and 800 s/mm<sup>2</sup>. The parameters were as follows: TR, 3,000 ms, TE, 49.5 ms, matrix, 128×96, field of view, 360×360 mm, 1.0 mm spacing, 5 mm slice thickness.

### Image analysis

Two radiologists (26 years and 6 years working experience) independently analyzed all images according to the 2013 Breast Imaging Reporting and Data System (BI-RADS) (13) at a workstation (Advantage windows Workstation 4.6; GE Healthcare) in a blinded way. Final decisions were made based on agreement of the two radiologists.

DCE-MRI: the morphology, internal enhancement characteristics, size, early enhancement rate (EER), and time-signal intensity curve (TIC) of the lesions were analyzed and recorded. For measurement of the TIC, a region of interest (ROI) smaller than the lesion was drawn on the largest portion of the tumor in the most obviously enhanced area of the lesion, avoiding the hemorrhagic and necrotic regions. When the measurements were repeated, the ROI size was consistent.

Lesion morphology: lesions were divided into three types: mass, NME, and mass combined with NME. The number of lesions was recorded. The size, shape, and margins of the mass were analyzed. Mass size: the maximum diameter of all tumors was measured on the workstation, and the average value was calculated after three measurements. According to a cutoff of 2 cm, the masses were divided into two groups, <2.0 and ≥2.0 cm, and the number was recorded. The shape (round, oval, or irregular) and margins (circumscribed, irregular, or spiculated) of the mass were recorded.

ADC value measurement: ADC measurement was performed in the GE workstation software. The area ROI was 0.8–7.9 cm<sup>2</sup> according to the lesion size. A single ROI was drawn on the lowest-signal area in the ADC maps that corresponded to the highest-signal focal in the DWI images. Subsequently, the ADC values were automatically calculated on ADC maps, with the location identical to that of the DWI image and DCE image. The ROI was smaller than the tumor and was drawn in the solid area of the lesion, avoiding the hemorrhagic and necrotic areas. When the measurements were repeated, the ROI size was consistent and might overlap (especially for the smaller tumors). The

ADC value was defined as the lowest ADC value of three or more measurements (*Figure 1A-1D*, *Figure 2A-2D*).

### Pathological analysis

All cases were confirmed by surgery or biopsy, and histopathologic diagnoses included histological type, grade, and molecular typing. Histological grade was assessed with the use of Nottingham modification of the Bloom-Richardson system, and the scores of grades I, II, and III were 3–5, 6–7, and 8–9, respectively (14). The assessment of progesterone receptor (PR), estrogen receptor (ER), and Ki-67 was carried out using the technique of avidin-biotin complex immunohistochemistry (IHC). At least 1% of the nuclei in ten high-power fields showed positive staining, which was considered ER and PR positivity. HER2 status was evaluated using IHC analysis and fluorescence *in situ* hybridization (FISH). The IHC 3+ or 2+ staining with positive HER2 gene amplification on FISH defined as HER2+. HER2+ breast cancer was divided into HER2+/HR- [HER2 (+), ER (-), PR (-), any expression of Ki-67], HER2+/HR+ [HER2 (+), ER (+), any expression of PR, any expression of Ki-67] (3). The pathological data of all patients were evaluated by two pathologists. In cases of differences of opinion, an agreement was reached through discussion and a diagnosis was made.

### Statistical analysis

The statistical analysis was performed using commercial software (IBM SPSS Statistics 25.0, Chicago, IL, USA). According to the normal distribution (using the Kolmogorov-Smirnov test), the data were expressed as the mean ± SD, otherwise the data were expressed as [M (Q1, Q3)]. Comparisons of counting data were made by the chi-square test *t* or Fisher's exact probability method. The Independent-Sample *t*-test or the non-parametric Mann-Whitney *U* test was used to compare measurement data. The binary logistic regression analysis was performed to determine DCE-MRI combined with ADC value for diagnosing HER2/HR- breast cancer. Receiver operating characteristic (ROC) curve analysis was used to analyze the diagnostic value of the ADC values, DCE-MRI and the combination of DCE-MRI and ADC value for HER2+/HR- breast cancer. Delong's test was used to compare the AUCs of the ADC value, DCE-MRI, and DCE-MRI combined with ADC value. P value <0.05 was considered significant.

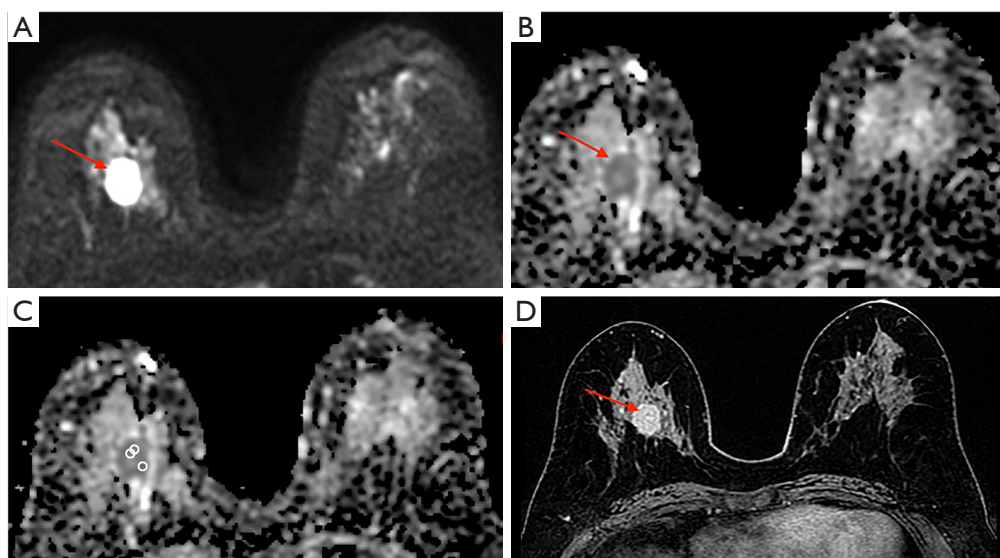


**Figure 1** HER2+/HR- breast carcinoma (IDC, histological grade III) in a 40 years old female. (A) DWI shows limited diffusion and a high signal (arrow). (B) On the ADC map, the tumor displays a low signal area (arrow). (C) On the ADC map, a single ROI was manually placed with the lesion. The measurement was repeated three or more times and the ADC values were automatically generated, which were  $1.26 \times 10^{-3}$ ,  $1.28 \times 10^{-3}$ ,  $1.30 \times 10^{-3}$  mm<sup>2</sup>/s, respectively. The ADC value of the tumor was determined as  $1.26 \times 10^{-3}$  mm<sup>2</sup>/s. (D) Contrast-enhanced axial T1-weighted MR image shows a slight heterogeneously enhancing round tumor with the diameter measuring 2.1 cm in the inner-upper right breast (arrow). HER2+/HR-, human epidermal growth factor 2 positive/hormone receptor negative; IDC, invasive ductal carcinoma; DWI, diffusion weighted imaging; ADC, apparent diffusion coefficient; ROI, region of interest; MR, magnetic resonance.

## Results

### *Pathological type and grade of HER2+ breast carcinoma*

Among 259 patients with HER2+ breast carcinoma, 96 were HR- and 163 were HR+. Pathological type and histological grade of HER2+/HR- and HER2+/HR+ breast tumors did not differ significantly ( $P=0.425$ ,  $P=0.083$ ; *Table 1*).

### *DCE-MRI and HER2+/HR- breast carcinoma*

The DCE-MRI findings of 259 HER2+ breast carcinoma patients are shown in *Table 2*. The morphology of tumors was related to HR status ( $P<0.001$ ), namely, HER2+/HR- breast cancers presented as NME or mass with NME, whereas HER2+/HR+ breast cancers presented as mass. The internal enhancement characteristics, EER, and TIC of lesions were not related to HR ( $P=0.514$ ,  $P=0.461$ ,  $P=0.524$ ).

Among 259 cases of HER2+ breast cancer, 190 (73.36%) showed a mass. *Table 3* shows the relationships between the size, shape, and margins of the mass and HR receptor status. The size of the mass was not correlated to HR status ( $P=0.557$ ), whereas the shape and margins were correlated to HR status ( $P=0.001$ ,  $P=0.028$ ). HER2+/HR- breast

carcinomas were more likely to be oval or round with circumscribed margins compared with HER2+/HR+ breast tumors (*Figures 1D, 2D*).

### *ADC value and HER2+/HR- breast carcinoma*

The ADC values of HER2+/HR- and HER2+/HR+ tumors were  $[1.2 (1.14, 1.33)] \times 10^{-3}$  mm<sup>2</sup>/s and  $[1.0 (0.89, 1.11)] \times 10^{-3}$  mm<sup>2</sup>/s, respectively, and the difference was significant ( $Z = -9.119$ ,  $P<0.001$ ) (*Figure 3A*).

ROC analysis showed that the ADC value was significant in diagnosing HER2+/HR- breast cancer, and the area under the curve (AUC) was 0.839 (95% CI: 0.791–0.887) ( $P<0.01$ ). The NPV, sensitivity and specificity were 89.8%, 86.5% and 70.6%, respectively, with the cut-off point of  $1.095 \times 10^{-3}$  mm<sup>2</sup>/s (*Figure 3B, Table 4*). These results suggest that the ADC values have diagnostic value for HER2+/HR- breast cancer.

### *DCE-MRI combined with ADC value and HER2+/HR- breast carcinoma*

The ROC curves of ADC value, DCE-MRI, and DCE-

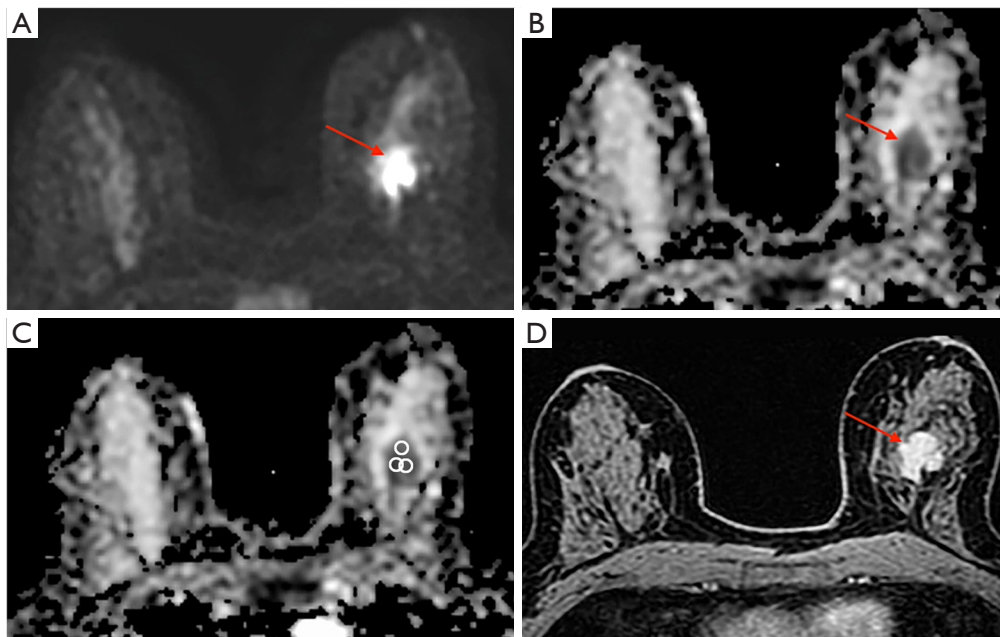


**Figure 2** HER2+/HR+ breast carcinoma (IDC, histological grade III) in a 55 years old female. (A) DWI shows limited diffusion and a high signal (arrow). (B) On the ADC map, the tumor displays a low signal area (arrow). (C) On the ADC map, a single ROI was manually placed with the lesion. The measurement was repeated three or more times and the ADC values were automatically generated, which were  $0.88 \times 10^{-3}$ ,  $0.95 \times 10^{-3}$ ,  $1.01 \times 10^{-3}$   $\text{mm}^2/\text{s}$ , respectively. The ADC value of the tumor was determined as  $0.88 \times 10^{-3}$   $\text{mm}^2/\text{s}$ . (D) Contrast-enhanced axial T1-weighted MR image shows a heterogeneously enhancing irregular tumor with the diameter measuring 2.0 cm in the central left breast (arrow). HER2+/HR+, human epidermal growth factor 2 positive/hormone receptor positive; IDC, invasive ductal carcinoma; DWI, diffusion weighted imaging; ADC, apparent diffusion coefficient; ROI, a region of interest; MR, magnetic resonance.

**Table 1** Relationship between HER2+ breast cancer and pathological type and grade

Pathologic type/grade	N	HER2+		$\chi^2$	P
		HR-	HR+		
Type					0.425
IDC	170	60	110		
IDC, DCIS	59	21	38		
DCIS	27	14	13		
ILC	1	0	1		
MC	2	1	1		
Grade				4.981	0.083
I	14	8	6		
II	136	43	93		
III	109	45	64		

IDC, invasive ductal carcinoma; DCIS, ductal carcinoma in situ; ILC, invasive lobular carcinoma; MC, mucinous carcinoma; HR, hormone receptor; HER2+, human epidermal growth factor 2 positive.

**Table 2** MRI dynamic enhancement characteristics of HER2+ breast cancer

Features	N	HER2+		$\chi^2$	P
		HR-	HR+		
Abnormal enhancement				46.908	<0.001
Mass	190	47	143		
NME	20	13	7		
Mass with NME	49	36	13		
Internal enhancement characteristics				1.395	0.514
Rim enhancement	24	11	13		
Heterogeneous	233	84	149		
Homogeneous	2	1	1		
Initial enhancement phase				1.561	0.461
Slow	21	6	15		
Medium	177	70	107		
Fast	61	20	41		
Delayed phase				1.351	0.524
I	5	3	2		
II	102	36	66		
III	152	57	95		

MRI, magnetic resonance imaging; HR, hormone receptor; HER2+, human epidermal growth factor 2 positive; NME, non-mass enhancement.

**Table 3** Size, shape and margin of HER2+ breast cancer with mass

Features	N	HER2+		$\chi^2$	P
		HR-	HR+		
Size				0.345	0.557
<2.0 cm	94	25	69		
$\geq$ 2.0 cm	96	22	74		
Shape				13.401	0.001
Round	9	5	4		
Oval	11	7	4		
Irregular	170	35	135		
Margin				7.156	0.028
Circumscribed	15	8	7		
Irregular	87	17	60		
Spiculated	98	22	76		

HER2+, human epidermal growth factor 2 positive; HR, hormone receptor.

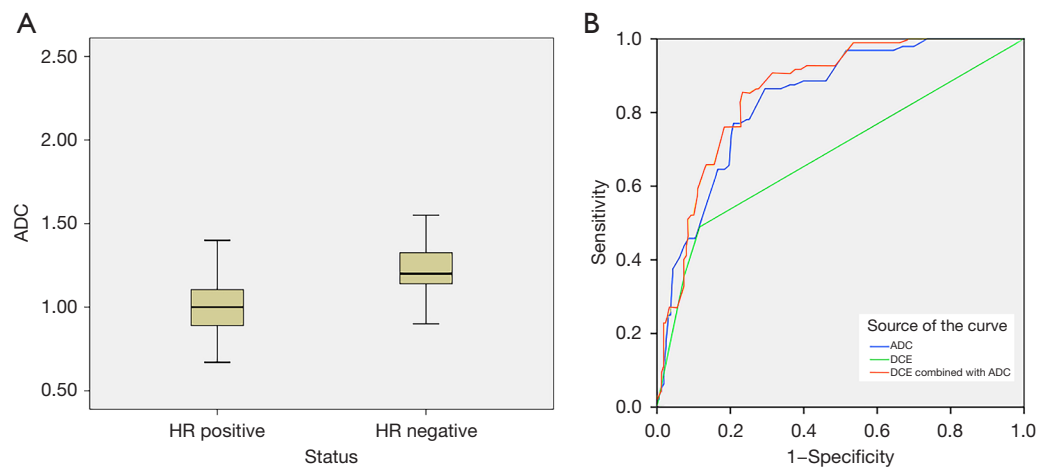


**Figure 3** Box plot of ADC value and ROC curve analysis. (A) Boxplots illustrating a comparison of the ADC value between HER2+/HR+ and HER2+/HR- breast carcinoma. (B) ROC analysis indicates that the ADC value is important for diagnosing HER2+/HR- breast carcinoma, with the threshold value of  $1.095 \times 10^{-3} \text{ mm}^2/\text{s}$  (NPV of 89.8%, sensitivity of 86.5% and specificity of 70.6%). AUCs of ADC value, DCE-MRI, DCE-MRI combined with ADC value were 0.839 (95% CI: 0.791–0.887), 0.689 (95% CI: 0.619–0.760), 0.860 (95% CI: 0.816–0.905), respectively. The DCE-MRI combined with ADC value showed significantly higher AUC than DCE alone ( $P < 0.0001$ ). ADC, apparent diffusion coefficient; ROC, receiver operating characteristic; HR, hormone receptor; DCE, dynamic contrast-enhanced; HER2+/HR-, human epidermal growth factor 2 positive/hormone receptor negative; AUC, area under the curve; MRI, magnetic resonance imaging; CI, confidence interval.

**Table 4** DCE-MRI and ADC values in diagnosing HER2+/HR- breast carcinoma

Parameters	AUC	NPV (%)	Sensitivity (%)	Specificity (%)
ADC	0.839	89.8	86.5	70.6
DCE	0.689	75.3	51.0	87.2
DCE combined with ADC	0.860	89.9	85.4	76.7

MRI, magnetic resonance imaging; HER2+/HR-, human epidermal growth factor 2 positive/hormone receptor negative; ADC, apparent diffusion coefficient; AUC, area under curve; DCE, dynamic contrast-enhanced; NPV, negative predictive value.

MRI combined with ADC value demonstrated AUCs (95% confidence interval) of 0.839 (0.791–0.887), 0.689 (0.619–0.760), 0.860 (0.816–0.905) (Figure 3B, Table 4). Although AUC of the DCE-MRI combined with ADC value showed no significantly difference from that of ADC ( $P = 0.0999$ ), AUC of the DCE combined with ADC was significantly higher than DCE alone ( $P < 0.0001$ ).

Using the optimal cut-off value for the DCE-MRI combined with ADC value resulted in NPV, sensitivity and specificity of 89.9%, 85.4% and 76.7%, respectively. Table 4 shows the NPV, sensitivity and specificity of each parameter.

## Discussion

Histological grade, size, and axillary lymph node status

are three major factors affecting the prognosis of breast carcinoma (15). Song *et al.* (8) showed that the histological grade of HER2+/HR- breast carcinoma was higher than that of HER2+/HR+ group. However, we found no statistically significant difference in histological grade between the two kinds of breast cancer ( $P = 0.083$ ), which may be due to the small number of HER2+/HR- breast cancers in our study. There was no statistical difference in gross pathology between the two groups of breast cancer ( $P = 0.425$ ). This study showed that HER2+/HR- and HER2+/HR+ breast carcinomas were not related to size ( $P = 0.557$ ), which was in line with previous research (8).

The DCE-MRI features of HER2+ breast cancer are irregular margins, multifocality, and an outflow curve (7); however, MRI features differ according to HR status. In

this study, HER2+/HR- breast cancers presented as NME or mass with NME, whereas HER2+/HR+ breast cancers presented as mass, and the difference was significant ( $P < 0.001$ ). There were few differences in the internal enhancement characteristics, early enhancement degree, and curve type of the lesions. HER2+/HR- breast tumors mostly had an oval or round shape with circumscribed margins compared with HER2+/HR+ breast tumors, which had an irregular mass and not circumscribed (irregular or spiculated) margins. The morphology and margins of HER2+ breast tumors differ with different HR status. There is no difference in hemodynamics of HER2+ breast carcinoma according to HR status (8,16). The present results and those of previous studies suggest that the morphology and margins of tumor are related to HR status, whereas the hemodynamic characteristics are not related to HR status, which is mainly determined by HER2 status. Therefore, HER2+/HR- breast carcinomas appear as NME, or mass with NME, and have a round or oval shape with circumscribed margins, whereas HER2+/HR+ breast cancers present as an irregular mass with not circumscribed (irregular or spiculated) margins.

The angiogenic ability of HER2+ breast cancer is stronger, and the tissue perfusion ability is faster than the increase of tumor cell density, and its ADC value is thus higher (17). The ADC values of HER2+/HR- and HER2+/HR+ breast cancers were  $[1.2 (1.14, 1.33)] \times 10^{-3} \text{ mm}^2/\text{s}$ , and  $[1.0 (0.89, 1.11)] \times 10^{-3} \text{ mm}^2/\text{s}$ , respectively, and there was statistical difference ( $Z = -9.119$ ,  $P < 0.001$ ). The reason for the decrease of ADC value in HER2+/HR+ breast cancer may be that HR expression inhibits angiogenesis, resulting in a decreased perfusion pathway, molecular diffusion limitation, and a decrease of ADC value (18). ROC analysis showed that the ADC value was important in diagnosing HER2+/HR- breast cancer, and the AUC was 0.839 (95% CI: 0.791–0.887) ( $P < 0.01$ ). The NPV, sensitivity and specificity were 89.8%, 86.5% and 70.6%, respectively, with the cut-off point of  $1.095 \times 10^{-3} \text{ mm}^2/\text{s}$ . This suggests that the ADC values have diagnostic value for HER2+/HR- breast cancer. In this study, the ADC value is measured three times or more times, and we chose the lowest ADC value, which reflects the most malignant part of the tumor (19,20). We have studied the measurement method of ADC value before and found that it is practical and convenient (21,22). Our results are inconsistent with the findings of You *et al.* (12), which may be due to different research methods and sample sizes. They found that the average values of ADC showed no significant difference in HER2 status differentiation through

the volumetric-tumor histogram-based analysis of intravoxel incoherent motion and non-Gaussian diffusion MRI.

In the study, the DCE-MRI features of breast cancer were only statistically different between the two groups in morphology, therefore, the combined diagnostic value of DCE-MRI and ADC value was analyzed by combining morphology and ADC value. Our research demonstrated that the diagnostic performance of the DCE-MRI combined with ADC value was good in diagnosing HER2+/HR- breast cancers, with an AUC of 0.860. ADC value showed diagnostic performance approaching the level of the DCE-MRI combined with ADC value (AUC of 0.839), compared to the DCE alone (AUC of 0.689).

The study had a number of limitations. First, the small number of samples, especially in HER2+/HR- breast cancers, may affect the universality of the results. Second, because the number of cases with axillary lymph node metastasis in this group was low, a statistical analysis of axillary lymph node status was not performed. Third, HER2+ breast cancer, which is mainly NME, was not evaluated because of the small number of samples in this research. The sample size needs to be expanded in the future. Fourth, the morphological evaluation of DCE-MRI and the ADC measurement were to some extent subjective, which may cause observational bias. Fifth, the results of the two observers were not tested for consistency, and there may be errors. Finally, the DCE-MRI features of breast cancer were only statistically different between the two groups in morphology, which may be due to the small sample.

## Conclusions

There are differences in morphology and ADC value between HER2+/HR- and HER2+/HR+ breast cancers. HER2+/HR- breast cancer presents as NME, or mass with NME, and has an oval or round shape with circumscribed margins, and the ADC value is higher than that of HER2+/HR+ breast cancer. The diagnostic performance of the DCE-MRI combined with ADC value was good in diagnosing HER2+/HR- breast cancers. MRI can be used as an effective tool in diagnosing HER2+/HR- breast carcinoma and could help clinicians select the optimal treatment and predict prognosis.

## Acknowledgments

We thank International Science Editing (<http://www.internationalscienceediting.com>) for the language editing of



this manuscript.

*Funding:* None.

## Footnote

*Conflicts of Interest:* All authors have completed the ICMJE uniform disclosure form (available at <https://qims.amegroups.com/article/view/10.21037/qims-22-1318/coif>). The authors have no conflicts of interest to declare.

*Ethical Statement:* The authors are accountable for all aspects of the work in ensuring that questions related to the accuracy or integrity of any part of the work are appropriately investigated and resolved. The study was conducted in accordance with the Declaration of Helsinki (as revised in 2013). The study was approved by the ethics committee of the Second Hospital of Shandong University [No. KYLL-2021(LW)042] and individual consent for this retrospective analysis was waived.

*Open Access Statement:* This is an Open Access article distributed in accordance with the Creative Commons Attribution-NonCommercial-NoDerivs 4.0 International License (CC BY-NC-ND 4.0), which permits the non-commercial replication and distribution of the article with the strict proviso that no changes or edits are made and the original work is properly cited (including links to both the formal publication through the relevant DOI and the license). See: <https://creativecommons.org/licenses/by-nc-nd/4.0/>.

## References

- Konat-Bąska K, Matkowski R, Błaszczuk J, Błaszczuk D, Staszek-Szewczyk U, Piłat-Norkowska N, Maciejczyk A. Does Breast Cancer Increasingly Affect Younger Women? *Int J Environ Res Public Health* 2020.
- Loibl S, Gianni L. HER2-positive breast cancer. *Lancet* 2017;389:2415-29.
- Cardoso F, Senkus E, Costa A, Papadopoulos E, Aapro M, André F, et al. 4th ESO-ESMO International Consensus Guidelines for Advanced Breast Cancer (ABC 4)†. *Ann Oncol* 2018;29:1634-57.
- Gianni L, Eiermann W, Semiglazov V, Lluch A, Tjulandin S, Zambetti M, Moliterni A, Vazquez F, Byakhov MJ, Lichinitser M, Climent MA, Ciruelos E, Ojeda B, Mansutti M, Bozhok A, Magazzù D, Heinzmann D, Steineifer J, Valagussa P, Baselga J. Neoadjuvant and adjuvant trastuzumab in patients with HER2-positive locally advanced breast cancer (NOAH): follow-up of a randomised controlled superiority trial with a parallel HER2-negative cohort. *Lancet Oncol* 2014;15:640-7.
- Kreutzfeldt J, Rozeboom B, Dey N, De P. The trastuzumab era: current and upcoming targeted HER2+ breast cancer therapies. *Am J Cancer Res* 2020;10:1045-67.
- Li Z, Ai T, Hu Y, Yan X, Nickel MD, Xu X, Xia L. Application of whole-lesion histogram analysis of pharmacokinetic parameters in dynamic contrast-enhanced MRI of breast lesions with the CAIPIRINHA-Dixon-TWIST-VIBE technique. *J Magn Reson Imaging* 2018;47:91-6.
- Seyfettin A, Dede I, Hakverdi S, Düzel Asig B, Temiz M, Karazincir S. MR imaging properties of breast cancer molecular subtypes. *Eur Rev Med Pharmacol Sci* 2022;26:3840-8.
- Song SE, Bae MS, Chang JM, Cho N, Ryu HS, Moon WK. MR and mammographic imaging features of HER2-positive breast cancers according to hormone receptor status: a retrospective comparative study. *Acta Radiol* 2017;58:792-9.
- Partridge SC, McDonald ES. Diffusion weighted magnetic resonance imaging of the breast: protocol optimization, interpretation, and clinical applications. *Magn Reson Imaging Clin N Am* 2013;21:601-24.
- McDonald ES, Hammersley JA, Chou SH, Rahbar H, Scheel JR, Lee CI, Liu CL, Lehman CD, Partridge SC. Performance of DWI as a Rapid Unenhanced Technique for Detecting Mammographically Occult Breast Cancer in Elevated-Risk Women With Dense Breasts. *AJR Am J Roentgenol* 2016;207:205-16.
- Surov A, Chang YW, Li L, Martincich L, Partridge SC, Kim JY, Wienke A. Apparent diffusion coefficient cannot predict molecular subtype and lymph node metastases in invasive breast cancer: a multicenter analysis. *BMC Cancer* 2019;19:1043.
- You C, Li J, Zhi W, Chen Y, Yang W, Gu Y, Peng W. The volumetric-tumour histogram-based analysis of intravoxel incoherent motion and non-Gaussian diffusion MRI: association with prognostic factors in HER2-positive breast cancer. *J Transl Med* 2019;17:182.
- Pinker K, Bickel H, Helbich TH, Gruber S, Dubsky P, Pluschnig U, Rudas M, Bago-Horvath Z, Weber M, Trattning S, Bogner W. Combined contrast-enhanced magnetic resonance and diffusion-weighted imaging reading adapted to the "Breast Imaging Reporting and Data System" for multiparametric 3-T imaging of breast lesions. *Eur Radiol* 2013;23:1791-802.

14. Elston CW. Classification and grading of invasive breast carcinoma. *Verh Dtsch Ges Pathol* 2005;89:35-44.
15. Rakha EA, Reis-Filho JS, Baehner F, Dabbs DJ, Decker T, Eusebi V, Fox SB, Ichihara S, Jacquemier J, Lakhani SR, Palacios J, Richardson AL, Schnitt SJ, Schmitt FC, Tan PH, Tse GM, Badve S, Ellis IO. Breast cancer prognostic classification in the molecular era: the role of histological grade. *Breast Cancer Res* 2010;12:207.
16. Bae MS, Seo M, Kim KG, Park IA, Moon WK. Quantitative MRI morphology of invasive breast cancer: correlation with immunohistochemical biomarkers and subtypes. *Acta Radiol* 2015;56:269-75.
17. Aydin H, Guner B, Esen Bostanci I, Bulut ZM, Aribas BK, Dogan L, Gulcelik MA. Is there any relationship between adc values of diffusion-weighted imaging and the histopathological prognostic factors of invasive ductal carcinoma? *Br J Radiol* 2018;91:20170705.
18. Ab Mumin N, Ramli Hamid MT, Wong JHD, Rahmat K, Ng KH. Magnetic Resonance Imaging Phenotypes of Breast Cancer Molecular Subtypes: A Systematic Review. *Acad Radiol* 2022;29 Suppl 1:S89-S106.
19. Jeong S, Kim TH. Diffusion-weighted imaging of breast invasive lobular carcinoma: comparison with invasive carcinoma of no special type using a histogram analysis. *Quant Imaging Med Surg* 2022;12:95-105.
20. Tuan Linh L, Minh Duc N, Minh Duc N, Tra My TT, Viet Bang L, Cong Tien N, Minh Thong P. Correlations between apparent diffusion coefficient values and histopathologic factors in breast cancer. *Clin Ter* 2021;172:218-24.
21. Zhao S, Guo W, Tan R, Chen P, Li Z, Sun F, Shao G. Correlation between minimum apparent diffusion coefficient values and the histological grade of breast invasive ductal carcinoma. *Oncol Lett* 2018;15:8134-40.
22. Zhao S, Shao G, Chen P, Li L, Yang Y, Zhao X, Guo W. Diagnostic performance of minimum apparent diffusion coefficient value in differentiating the invasive breast cancer and ductal carcinoma in situ. *J Cancer Res Ther* 2019;15:871-5.

**Cite this article as:** Chen P, Zhao S, Guo W, Shao G. Dynamic contrast-enhanced magnetic resonance imaging features and apparent diffusion coefficient value of HER2-positive/HR-negative breast carcinoma. *Quant Imaging Med Surg* 2023;13(8):4816-4825. doi: 10.21037/qims-22-1318